

January 2015

Bayesian Spatial Modeling Of Respiratory Syncytial Virus Transmission In The United States

Samantha Emanuele

Yale University, samantha.emanuele@yale.edu

Follow this and additional works at: <http://elischolar.library.yale.edu/ysphtdl>

Recommended Citation

Emanuele, Samantha, "Bayesian Spatial Modeling Of Respiratory Syncytial Virus Transmission In The United States" (2015). *Public Health Theses*. 1077.

<http://elischolar.library.yale.edu/ysphtdl/1077>

This Open Access Thesis is brought to you for free and open access by the School of Public Health at EliScholar – A Digital Platform for Scholarly Publishing at Yale. It has been accepted for inclusion in Public Health Theses by an authorized administrator of EliScholar – A Digital Platform for Scholarly Publishing at Yale. For more information, please contact elischolar@yale.edu.

Bayesian Spatial Modeling of RSV Transmission in the United States
Master of Public Health in Biostatistics Thesis

Candidate: Samantha Emanuele

Advisors: Virginia Pitzer Sc.D.¹, Joshua Warren Ph.D.²

¹ Department of Epidemiology of Microbial Diseases, Yale School of Public Health ² Department of Biostatistics, Yale School of Public Health

Abstract

Respiratory syncytial virus (RSV) is a common virus infecting the respiratory system and can cause severe disease in vulnerable populations. It has been shown that the RSV epidemic in the United States is seasonal, peaking in late fall in Florida and a few months later in the upper Midwest. Although a seasonal trend has been described, it is still unclear if there are any spatial trends between states. For this paper, RSV laboratory data from the continental United States was used to model the transmission dynamics of RSV in each state. We conducted an explanatory analysis to investigate the presence of spatial autocorrelation in parameters describing RSV transmission between states using a two-stage approach. In stage one we estimated the parameters using a dynamic mathematical model. In stage two we utilized Bayesian methods, where we considered two modeling options: spatial independence and spatial correlation. To model spatial correlation, we included a state-specific spatial parameter $w(s_i)$, where $w(s_i)$ is assigned the intrinsic conditional autoregressive (CAR) model. The two models were compared to determine if spatial correlation is present in the data. The seasonal offset and amplitude of seasonality in transmission rate parameters both showed spatial autocorrelation in preliminary analyses. Spatial modeling, using stage two, was implemented for these two parameters. The spatial model showed that spatial correlation was present in the data for the seasonal offset and amplitude of seasonality parameters, suggesting the need to account for spatial correlations in future work.

Table of Contents

| | |
|--------------------|----|
| Tables..... | 3 |
| Figures | 4 |
| Introduction | 7 |
| Methods | 8 |
| Results | 13 |
| Discussion | 14 |
| References | 20 |
| Appendix | 22 |

Tables

| Parameter Estimate | Moran's Index (p-value) |
|--------------------|----------------------------|
| R_0 | 0.094 (0.10) |
| b | 0.168 (0.02) |
| ϕ | 0.54 (< 0.001) |
| h | 0.11 (0.06) |

Table 1 Explanatory Analysis The Moran's I test was conducted for all four parameters. The test statistic and p-value are recorded above. Only parameters that were statistically significant at $\alpha = 0.05$ significant level were further explored

| Prior | Seasonal Offset | Amplitude of Seasonality |
|---------------------|----------------------|--------------------------|
| Gamma(0.1, 0.1) | 0.87 (0.72, 0.96) | 0.55 (0.18, 0.90) |
| Gamma(0.01, 0.01) | 0.95 (0.83, 0.99) | 0.49 (0.05, 0.96) |
| Gamma(0.001, 0.001) | 0.87 (0.72, 0.96) | 0.46 (0.01, 0.99) |
| Uniform(0, 1000) | 0.89 (0.73, 0.99) | 0.51 (0.09, 0.90) |

Table 2 Sensitivity Analysis of Prior Distributions Each of the four prior distributions was used to calculate the proportion of spatial error for the seasonal offset and the amplitude of seasonality. The 95% credible intervals are in parentheses.

Figures

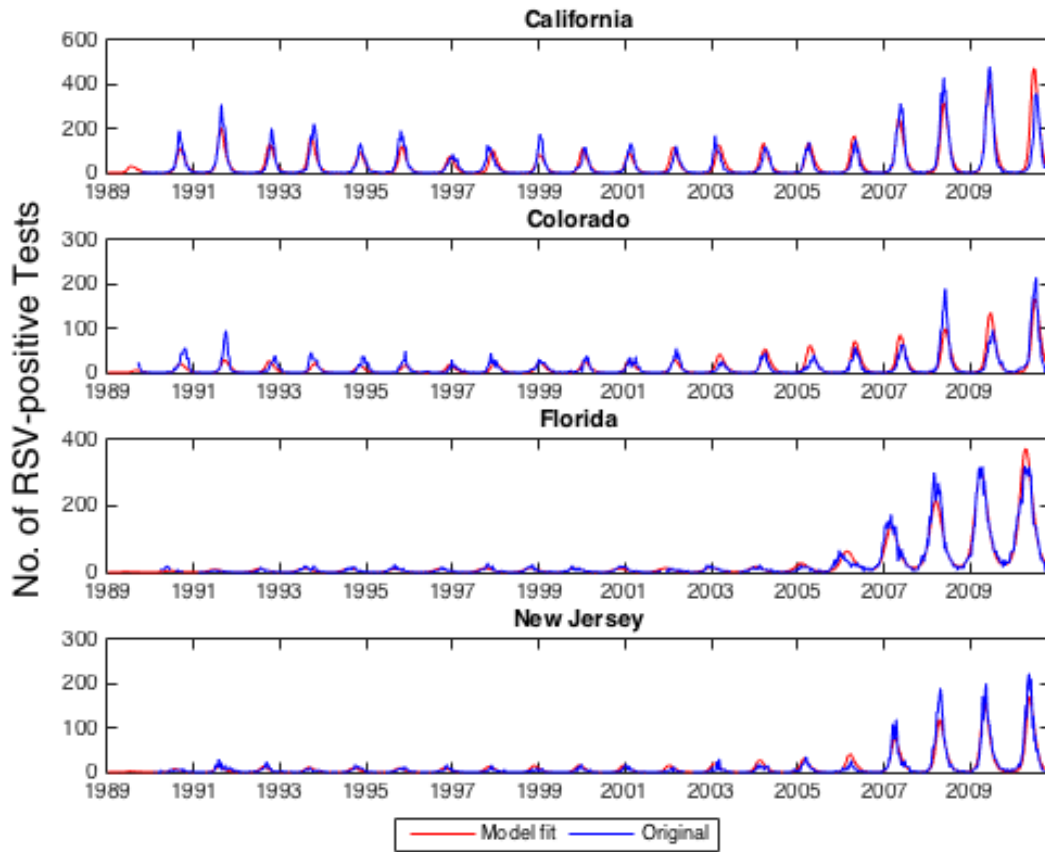


Fig. 1. Number of RSV positive Tests Time series of RSV-positive test by week from 1989 – 2010 in four select states. These states represent different areas within the United States, West Coast, Midwest, Southeast and Northeast. The blue line is the laboratory data from NREVSS and the red line is the best-fit dynamic model output.

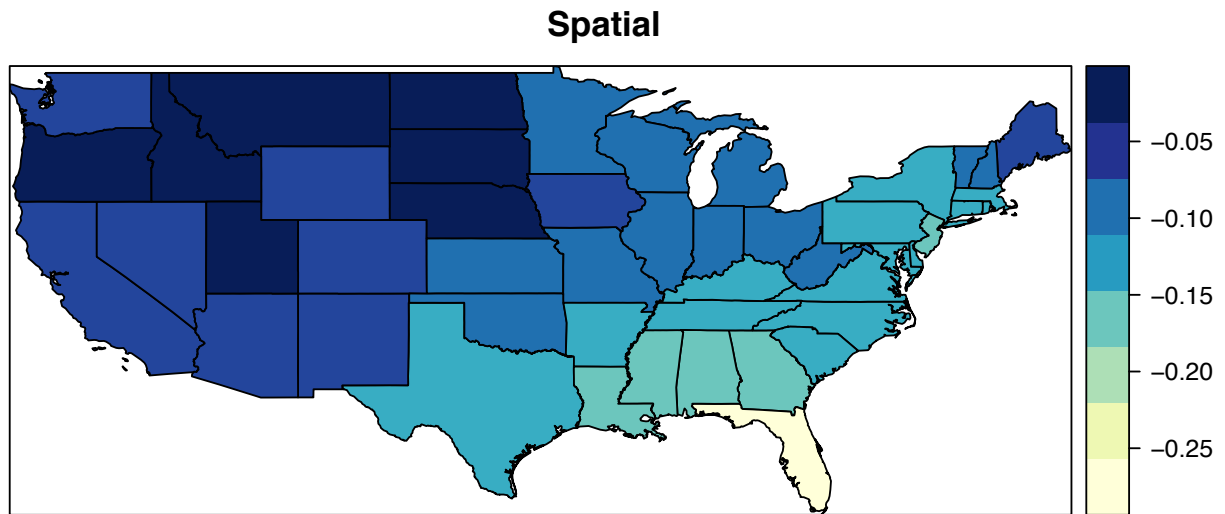
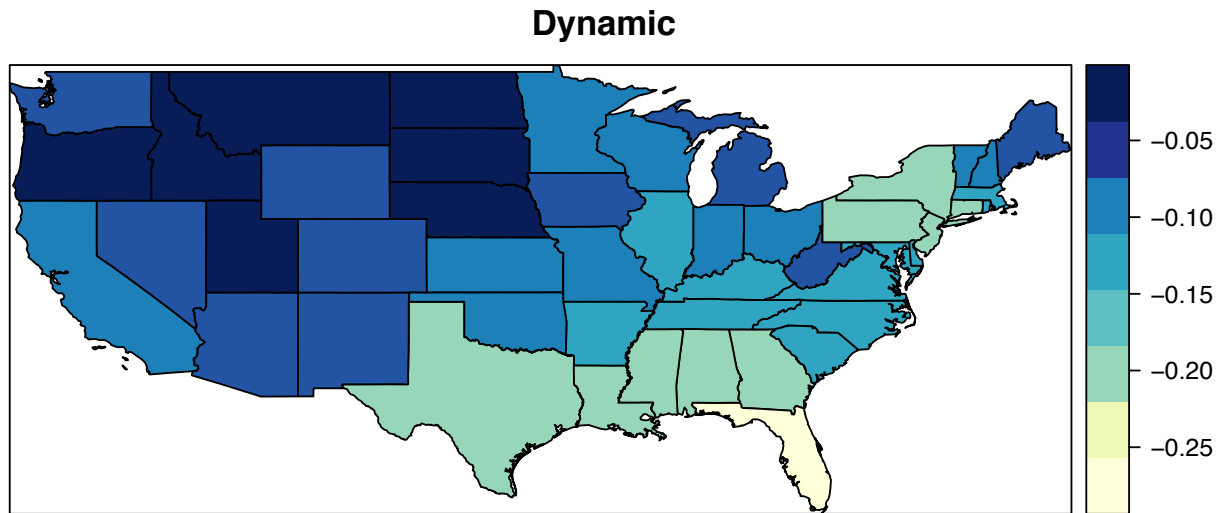


Fig. 2. Seasonal offset by State Estimates of the seasonal offset parameter for each state. The top plot is the estimates obtained from the dynamic model and the bottom is from the spatial model

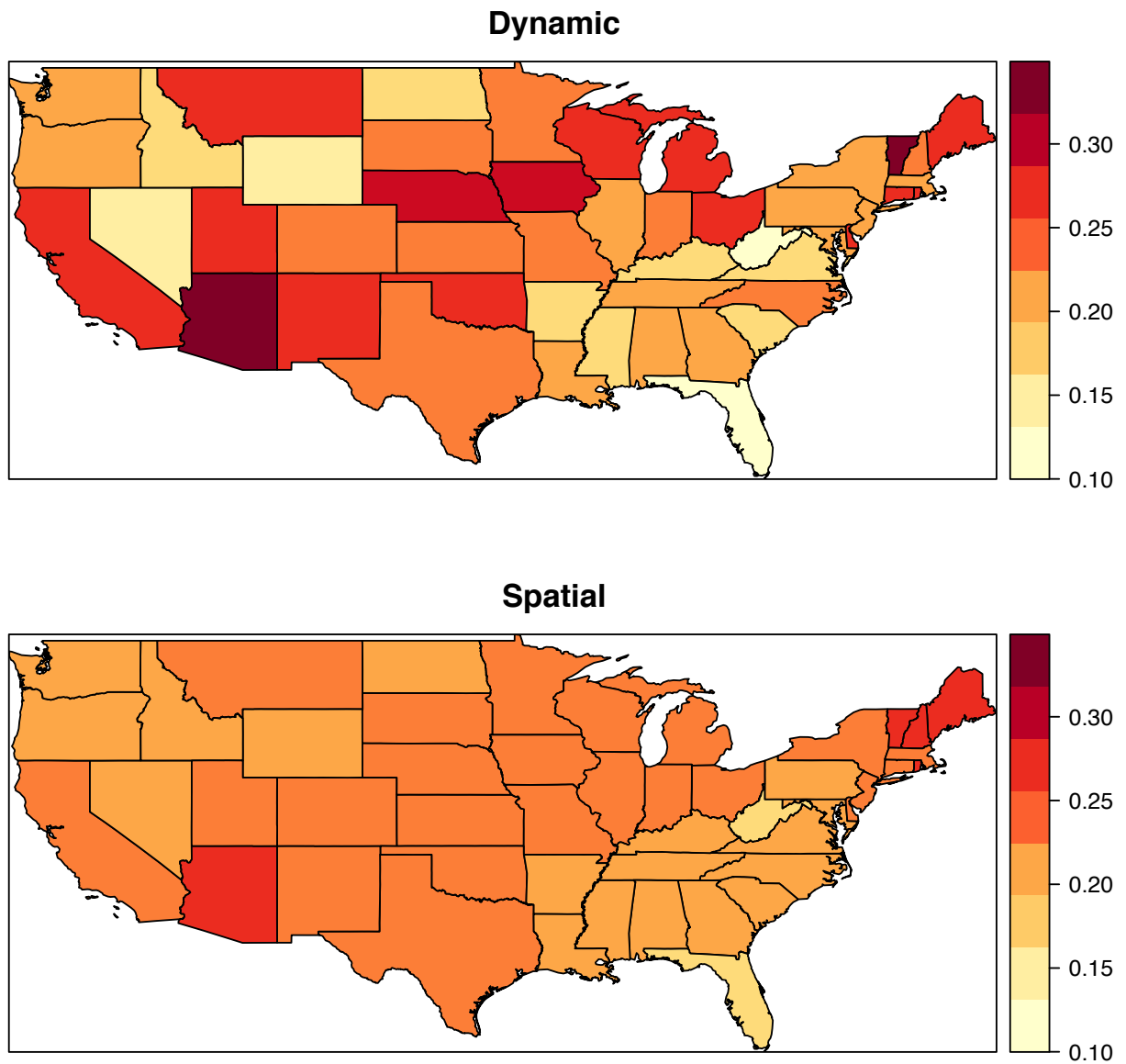


Fig. 3. Amplitude of Seasonality by State Estimates of the amplitude of seasonality parameter (b) for each state. The top graph is the estimates obtained from the dynamic model and the bottom is from the spatial model.

Introduction

Respiratory syncytial virus (RSV) is a common virus infecting the respiratory system, specifically the lungs and breathing passageway. Infection occurs throughout life, but disease due to RSV is most common in young infants and the elderly population [1]. Although typically mild, RSV can be a serious virus for these vulnerable populations. For children younger than 5 years old, an estimated 66,000 – 199,000 deaths per year are attributed to RSV globally [2]. A majority of these deaths occurred in developing countries, but RSV still poses a serious threat in the United States. More than 2,000 hospitalizations for every 100,000 infants younger than 1 year old have been estimated to be caused by RSV each year in the United States [3].

RSV has been shown to have a seasonal component, specifically in the US and other temperate locations. Typically, incidences of RSV peak annually in the winter but the timing of peak incidence can range from early October in southern states, such as Florida, to May in states in the upper Midwest [4]. Various environmental drivers, such as vapor pressure, minimum temperature, precipitation, and potential evapotranspiration are correlated with seasonality parameters in RSV transmission [5].

Currently, the approved form of prevention for RSV is palivizumab prophylaxis for high-risk infants [6]. Although effective, this method is very costly and the timing of administration is important to maximize the cost-effectiveness, motivating the importance of understanding the seasonality of RSV [7].

Extensive research has been done to describe the seasonality of RSV, but it is still unclear if there are any spatial trends between states after accounting for differences in transmission [8-10]. The purpose of this paper is to explore potential spatial trends in the transmission dynamics of RSV across the continental US. Discovering insights regarding spatial trends in RSV

transmission is important for understanding the seasonality of this epidemic and for determining the optimal timing for prophylaxis.

Methods

Data

The data used for this analysis consisted of laboratory reporting data from the National Respiratory and Enteric Virus Surveillance System (NREVSS) and demographic data from the US Census Bureau and Center for Disease Control (CDC). The laboratory data reported the weekly number of positive RSV tests and total number of RSV tests performed by state from July 1989 to May 2010. Positive RSV specimens were detected using the following three methods: antigen detection, reverse transcription chain reaction and viral culture. This data is voluntarily reported each week by participating laboratories, resulting in non-consistent data for different states over time [11]. A scaling factor was therefore calculated for each state by taking the two-year moving average of the number of RSV tests reported each week divided by the average number of tests per week for the entire period of consistent reporting [5]. This scaling factor was then multiplied by the model output for each state. The demographic data consisted of an initial population size and crude annual birth rate for each state [12-13].

Dynamic Model

The RSV laboratory data was fitted to an age-adjusted Susceptible-Infectious-Recovered-Susceptible (SIRS)-like model developed by Pitzer et al. to model the transmission dynamics of RSV for each of the 49 states (excluding Alaska and Hawaii, and including District of Columbia)[5]. The SIRS model assumes infants are born with maternal immunity, which wanes

exponentially with a mean duration of 16 weeks, leaving the infant fully susceptible to RSV infection. It is assumed that an individual will build partial immunity with each infection of RSV. This partial immunity reduces both the risk of subsequent infection and the duration of such infections. Furthermore, both age and number of infections influence the risk of developing severe respiratory disease; we assume a fraction h of these severe cases are reported in our data [5]. The reporting fraction is assumed to vary by state, and is essentially a nuisance parameter, since reporting was voluntary and inconsistent across states.

The rate of transmission of RSV from infectious to susceptible individuals (λ) is assumed to vary seasonally according to a sinusoidal seasonal forcing function:

$$\lambda = \beta_0(1 + b * \cos(2\pi(t - \phi)))I$$

where

$$I = I_1 + \rho_1 I_2 + \rho_2 (I_3 + I_4)$$

In the above equation, b and ϕ represent the amplitude of seasonality and the seasonal offset.

The basic reproductive number (R_0) for this model is given by $R_0 = \beta_0/\gamma_1$, where β_0 is the transmission matrix and γ_1 is the removal rate. R_0 was calculated using the next generation matrix method created by van den Driessche and Watmough [14].

Stage 1

We fit the model to the laboratory data to estimate the mean transmission rate as indicated by the basic reproductive number (R_0), amplitude of seasonality (b), seasonal offset (ϕ), and proportion of hospitalizations that are reported (h) for each state. The seasonal offset parameter describes the peak timing of RSV transmission as a fraction of the year and can vary between -0.5 and 0.5. A seasonal offset of 0 implies that the peak transmission occurs on January

1st and -0.5 and 0.5 correspond to a peak time of July 1st [5]. The laboratory data did not contain information on the age of cases, which is an important detail for estimating reliable values of R_0 [5]. Therefore, a normal prior with mean 8.9 and variance 0.2 for the estimate R_0 value for each state was added to the likelihood estimation framework for the dynamic model, based on the estimated variation in R_0 for 10 states with age-specific hospitalization data [5]. The best-fit model parameters for each state were determined by maximizing the likelihood of the dynamic model output given the data. This likelihood was calculated by assuming a Poisson distribution for the number of positive RSV tests per week, x_w , with mean \hat{x}_w , where \hat{x}_w is the number of severe respiratory infections predicted from the model multiplied by the reporting fraction [5]. Using the ‘fminsearch’ command in MATLAB, the parameter estimates were obtained by minimizing the negative log-likelihood for each of the 49 models.

Spatial Exploration

For this paper, we defined the spatial structure using a neighborhood approach, where a state was considered a neighbor if their borders touch. For example, Alabama has neighbors, Georgia, Mississippi, Florida and Tennessee. The spatial weights matrix was a matrix of 0’s and 1’s, where entry $W_{i,j} = 1$ when state i and j are neighbors.

Parameter estimates describing the variation in transmission between states were first examined for any spatial autocorrelation using a Moran’s I test. Parameter estimates were considered to be statistically significant at $\alpha = 0.05$ significance level. The parameter estimates that showed spatial trends were then modeled in stage two, first using a non-spatial model and then comparing the results to a spatial model. Both models were fit using Markov chain Monte Carlo (MCMC) methods, which were executed through OpenBUGS. Each MCMC simulation

was run with 3 chains for 100,000 iterations and a burn-in length of 50,000 iterations based on visual inspection of the trace plots and assessment of Monte Carlo standard errors for the posterior means.

The parameter estimates that were analyzed were $\phi(s_i)$ and $b(s_i)$, where $\phi(s_i)$ is the seasonal offset parameter for state s_i , (i ranging from 1 to 49), and $b(s_i)$ is the amplitude of seasonality for state s_i . All states were included with the exception of Alaska and Hawaii, and the inclusion of the District of Columbia.

Stage 2

In stage 2A, we used a baseline model to be later compared with the spatial model.

Below is the baseline model

$$\phi(s_i) \stackrel{\text{iid}}{\sim} N(\mu, \sigma^2)$$

where $\phi(s_i)$ is assumed to be normally distributed with mean μ and variance σ^2 . μ is given a flat prior distribution to allow the data to drive the inference rather than our prior beliefs and σ^2 is assumed to follow an approximately inverse gamma prior distribution with shape and scale parameters both equal to 0.1.

In stage 2B, spatially correlated parameters $w(s_i)$ are added to the model, where $w(s_i)$ is modeled by the intrinsic conditional autoregressive (CAR) model [15]. The CAR model is a prior distribution for random effects where the conditional mean is a weighted sum of its neighbors and the variance depends on the total number of neighbors [16]. Regions with more neighbors have a smaller prior variance compared to regions with fewer neighbors.

$$\phi(s_i) = \mu + w(s_i) + \epsilon(s_i)$$

The above model has two pieces of variability: spatial ($\sigma_{spatial}^2$) and non-spatial (σ_{ϵ}^2). When the spatial variance is equal to zero, we end up with the non-spatial model. The $\epsilon(s_i)$ values are normally distributed with mean 0 and variance σ_{ϵ}^2 , which has a prior distribution of inverse gamma with shape and scale parameters equal to 0.1. This variance represents the non-spatial variability. The prior distribution for the spatial variance is also inverse gamma with shape and scale parameters equal to 0.1. Similar to stage 2A, the prior distribution for μ is a flat distribution.

We conducted a sensitivity analysis to determine the sensitivity of the results to different choices of prior distributions (Table 1). The sensitivity analysis revealed that the results were generally robust to the choice of prior distribution, confirming our decision to use an inverse gamma distribution with shape and scale parameters equal to 0.1.

Model 2A and model 2B were compared to determine if some of the variability in the estimates could be explained by the addition of a spatially correlated parameter. The models were compared using the proportion of spatial variance compared to the total variance, where the total variance is the sum of spatial variance and noise.

$$Prop = \frac{\sigma_{spatial}^2}{\sigma_{spatial}^2 + \sigma_{\epsilon}^2}$$

When the proportion is close to 1, this suggests that most of the variability can be explained by the spatial correlation between states. However, if the variance of the spatial model is close to 0, then the above equation would approach 0. Proportions close to 0 suggest that most of the variability in the estimates is due to spatially independent errors.

Results

Laboratory Data

The laboratory data had a total of 1087 weeks worth of data, where the number of weekly reported data varied state by state. No state had data for all 1087 weeks; Louisiana was the closest with a total of 1084 weeks of reported data. Various states had minimal data, such as Vermont, who only had 187 weeks of reported data. The average number of weekly data across all 49 states was 875 weeks and had a standard deviation of 207.69 (Table S1). The number of positive tests per week also varied state by state. Some states had an average of 1 positive test per week (District of Columbia), while others had an average of 64 positive tests per week (Texas) (Table S1).

Dynamic Model

The dynamic model was able to capture the observed seasonality of RSV based on the laboratory data for each state (Fig. 1). For the 49 states, the average estimated R_0 was 9.097, and ranged from 8.5 – 9.59. The amplitude of seasonality and the seasonal offset parameter had means of 0.2255 and -0.0974, respectively. The range of ϕ and b across the continental US can be seen in Fig. 2 and Fig. 3. Although h is hard to interpret as mentioned above, the average estimated value for all 49 states was 0.19 and ranged from 0.04 to 1.02. The parameter estimates for all 49 states are available in Table S2.

The seasonal offset parameter was shown to be spatially autocorrelated with a p-value <0.001. The Moran's index was 0.54, suggesting a clustering effect. The amplitude of seasonality was also spatially autocorrelated with a p-value = .024 and a Moran's index of 0.168. The p-values for R_0 (0.1) and h (0.06) were not statistically significant at $\alpha = 0.05$ significance

level, so these estimates were not further explored. The results from the Moran's I test are summarized in Table 1.

Seasonal Offset

The seasonal offset parameters were first modeled using a non-spatial model. This resulted in $\mu = -0.099$ and $\sigma^2 = 0.0078$. With the addition of the spatial parameter $w(s_i)$, μ remained the same and σ^2 increased to 0.046. The proportion of spatial variance compared to total variance is 0.87 (Table 2), meaning that 87% of the variation in the model is due to spatial variation. The parameter estimates from the spatial model are compared to the dynamic model in Fig. 2.

Amplitude of Seasonality

The same process was repeated for the amplitude of seasonality. With the non-spatial model, we saw a $\mu = 0.228$ and $\sigma^2 = 0.0069$. In the spatial model, μ stayed the same and σ^2 increased to 0.1667. The proportion of spatial variance compared to total variance is 0.54 (Table 2) meaning that approximately 54% of the variation in the model is due to spatial variation. The estimated b from the dynamic and spatial models is compared in Fig. 3.

Discussion

Understanding the spatiotemporal trends of RSV is essential for optimizing the timing of prophylaxis for high-risk infants [7]. With the use of spatial smoothing methods and mathematical modeling, we are able to learn more about the seasonality of RSV, specifically regarding the spatial patterns among seasonal parameters describing the transmission of RSV.

Dynamic Model

The dynamic model was able to capture the overall seasonality of RSV for each of the 49 states. The parameter estimates obtained for the transmission rate were consistent with the values seen in the literature [5, 17,18]. Our mean estimate of R_0 (9.097) was slightly higher compared to the mean R_0 obtained by Pitzer et al., however we fit all 49 states regardless of the quality of data while Pitzer et al. looked at a subset of states based on the consistency of data reported [5].

The seasonal offset parameter showed a clear spatial trend when plotted for each of the 49 states. The smallest seasonal offset parameter was for Florida, implying that RSV transmission peaks the earliest in this state. The map in Fig. 2 clearly shows the values of ϕ increasing as it moves northwest from Florida. Previous research suggests that the incidence of RSV peaks firsts in Florida and then later in the upper Midwest [4]. Although the research by McGuinness et al. looked at the timing of RSV cases rather than the timing of transmission, our research is consistent with these results. Despite the different analyses, it is plausible to see the same pattern of movement for both the timing of transmission and incidence since the incubation period of RSV is 2-8 days [19]. Studying the timing of transmission can help understand how

and why RSV spreads through the United States. Additionally, understanding the timing of transmission can help predict outbreaks of the epidemic.

The amplitude of seasonality parameter does not show as clear of a spatial trend compared to the seasonal offset parameter, but there are still important insights that can be gained from our analysis. Florida has the smallest amplitude of seasonality parameter and there appears to be some clustering effects around the Midwest, Southwest, and Northeast.

A significant Moran's I test confirmed the potential spatial correlation for both the seasonal offset and the amplitude of seasonality. Additionally, they both had a positive Moran's index, suggesting that there is a spatial clustering effect

Seasonal Offset

With the addition of the spatial parameter, we begin to see parameter estimates becoming more similar to their neighbors. For example, West Virginia becomes less of an outlier in the spatial model as its estimate begins to decrease towards its neighbors. Similarly, the estimates for New Jersey, New York, and Pennsylvania increase to become more like their neighbors in the spatial model. Another interesting observation is that Florida appears to be more of an outlier when accounting for spatial correlation. This is due to Florida's neighbors, Georgia and Alabama, having seasonal offset estimates closer to their neighbor, Tennessee's value. With the exception of Florida, the southernmost states (Texas, Louisiana, Alabama, Mississippi and Georgia) have estimates that shifted closer to estimates for the rest of the country.

Amplitude of Seasonality

Fig. 3 shows the estimates of the amplitude of seasonality in the spatial model becoming similar to their neighbors. This is especially true for states that were outliers in the dynamic model, such as Arizona and Vermont. In the dynamic model, the amplitude of seasonality did not appear to follow a clear spatial pattern for the middle of the US. With the spatial model there is a clear cluster of states with similar amplitude of seasonality estimates starting in Texas and working its way north to Wisconsin and Michigan. A few states that had estimates similar to Florida in the dynamic model have increased to become more like their neighbors. These states include Idaho, Nevada, Colorado, and West Virginia. Another interesting note is that the parameter estimate for Alabama decreased in the spatial model and shifted more towards Florida.

Connection Between Moran's I Test and Stage 2.

The results obtained from stage 2 are consistent with what we saw with the Moran's I test. For the seasonal offset parameter, we saw a p-value <0.001 from the Moran's I test and the proportion of variation due to spatial variance was 0.87. This suggests that there is a strong spatial trend for this parameter. Similarly, we saw a smaller p-value for the amplitude of seasonality, which was 0.024. The proportion of variance was also smaller in comparison to the seasonal offset parameter, suggesting less of a spatial trend. Our results from stage 2 are consistent with the Moran's I test, validating the methods and results of our analysis.

Relationship to Previous Studies

Pitzer et al. explored the relationship between various environmental drivers and the transmission dynamics of RSV. The seasonal offset parameter and amplitude of seasonality

were both found to be negatively correlated with vapor pressure, minimum temperature, and precipitation [5]. In contrast, we looked at the spatial trends of these two parameters and saw them increase as one moves north. With the assumption that northern states have lower minimum temperature, our results follow the theory that the seasonal offset parameter and amplitude of seasonality are negatively correlated with minimum temperature. Using the previous research, we begin to understand the spatial trends that are observed. Assuming neighboring states have similar environments, it makes sense to see that neighboring states have similar parameter estimates as well.

Limitations and Future Directions

A major limitation of this research is the variation of the RSV laboratory data for each state. As seen in Table S1 and Table S2, the total amount of weekly data reported and overall number of cases of RSV varies from state to state. This variation is likely to affect the overall fit of the dynamic model, especially for states with a biennial pattern of RSV transmissions, as it is difficult to capture these patterns. It is plausible that the variation we saw between the dynamic model and spatial model was due to the differences in the data.

Another limitation regarding the RSV laboratory data is that it did not contain age-specific information, which is an important factor for estimating the state-specific transmission rate, R_0 . Although we found that the estimates of R_0 were not spatially autocorrelated and thus the spatial analysis focused on the offset of seasonality and seasonal amplitude variable, all of the parameter estimates depend on one another. It is possible these estimates would have been improved with age-specific RSV data.

This analysis treated the estimates like data, meaning that we did not account for the uncertainty in the parameter estimates obtained from the dynamic model. In order to get accurate variances, likelihood profiles would have needed to be created, requiring the models for each of the 49 states to be refit for different values of ϕ and b . This process is both computationally intensive and time consuming, but we hope to consider it in future work.

Lastly, the way space was defined is a limitation. We only took into account the number of neighbors a state had, which varies across the US. For example, states in the Northeast are very close to each other, resulting in more neighbors, whereas states in the Midwest are further apart and may have fewer neighbors. Future work should consider other definitions of space, such as the total distance between states. Using what is known about environmental drivers and their affects on the transmission dynamics of RSV, future work should incorporate these environmental drivers into the way we define space. Additionally, it may be of interest to consider the migration and travel habits of American citizens. For example, residents in the Northeast may frequently travel to Florida during the winter months. It would be interesting to take account of these social habits when trying to determine the timing of transmission.

This paper used explanatory analysis to explore the need to account for spatial correlation in modeling the transmission dynamics of RSV. By first employing a Moran's I test, we saw a spatial correlation for the seasonal offset and amplitude of seasonality parameters. Using Bayesian methods we showed that spatial correlation is present in the data. This explanatory analysis provides evidence suggesting future model development should account for spatial correlation that exists between neighboring states.

References

1. Respiratory Syncytial Virus Infection (RSV). Available: <http://www.cdc.gov/rsv/>. Accessed 8 December 2014.
2. Nair H, Nokes DJ, Gessner BD, Dherani M, Madhi SA, et al. (2010) Global burden of acute lower respiratory infections due to respiratory syncytial virus in young children: A systematic review and meta-analysis. *Lancet* 375: 1545–1555. doi:10.1016/S0140-6736(10)60206-1.
3. Zhou H, Thompson WW, Viboud CG, Ringholz CM, Cheng P-Y, et al. (2012) Hospitalizations associated with influenza and respiratory syncytial virus in the United States, 1993-2008. *Clin Infect Dis* 54: 1427–1436. doi:10.1093/cid/cis211.
4. McGuinness CB, Boron ML, Saunders B, Edelman L, Kumar VR, et al. (2014) Respiratory syncytial virus surveillance in the United States, 2007-2012: results from a national surveillance system. *Pediatr Infect Dis J* 33: 589–594. doi:10.1097/INF.0000000000000257.
5. Pitzer VE, Viboud C, Alonso WJ, Wilcox T, Metcalf CJ, et al. (2015) Environmental Drivers of the Spatiotemporal Dynamics of Respiratory Syncytial Virus in the United States. *PLoS Pathog* 11(1): e1004591. doi:10.1371/journal.ppat.1004591
6. Modified recommendations for use of palivizumab for prevention of respiratory syncytial virus infections. *Pediatrics* 124: 1694–1701 doi:–10.1542/peds.2009–2345.
7. Panozzo CA, Stockman LJ, Curns AT, Anderson LJ (2010) Use of respiratory syncytial virus surveillance data to optimize the timing of immunoprophylaxis. *Pediatrics* 126: e116–23 doi:–10.1542/peds.2009–3221.
8. Gilchrist S, Török TJ, Gary HE, Alexander JP, Anderson LJ (1994) National surveillance for respiratory syncytial virus, United States, 1985–1990. *J Infect Dis* 170: 986–990. doi: 10.1093/infdis/170.4.986
9. Panozzo CA, Fowlkes AL, Anderson LJ (2007) Variation in timing of respiratory syncytial virus outbreaks: Lessons from national surveillance. *Pediatr Infect Dis J* 26: S41–5 doi:10.1097/INF.0b013e318157da82.
10. Bloom-Feshbach K, Alonso WJ, Charu V, Tamerius J, Simonsen L, et al. (2013) Latitudinal variations in seasonal activity of influenza and respiratory syncytial virus (RSV): a global comparative review. *PLoS One* 8: e54445 doi:10.1371/journal.pone.0054445.
11. CDC/NREVSS. RSV Surveillance Reports. Available: <http://www.cdc.gov/mmwr/preview/mmwrhtml/mm6035a4.htm>. Accessed 16 April

2015.

12. Population of States and Counties of the United States: 1790 to 1990 (n.d.). US Census Bur. Available: <http://www.census.gov/population/www/censusdata/pop1790-1990.html>. Accessed 4 April 2013.
13. CDC/NVSS (n.d.) Vital Statistics Online. Natl Vital Stat Syst. Available: <http://www.cdc.gov/nchs/nvss.htm>. Accessed 4 April 2013.
14. Van Den Driessche, P.; Watmough, J. (2002). "Reproduction numbers and sub-threshold endemic equilibria for compartmental models of disease transmission". *Mathematical Biosciences* **180** (1–2): 29–48. doi:10.1016/S0025-5564(02)00108-6. PMID 12387915. [edit](#)
15. Cressie, N. (1993). *Statistics for spatial data* (Rev. ed.). New York: Wiley.
16. Statistical Analysis Handbook. (n.d.). Available: http://www.statsref.com/HTML/index.html?car_models.html. Available 17 April 2015.
17. White LJ, Mandl JN, Gomes MGM, Bodley-Tickell AT, Cane PA, et al. (2007) Understanding the transmission dynamics of respiratory syncytial virus using multiple time series and nested models. *Math Biosci* 209: 222–239 doi:10.1016/j.mbs.2006.08.018.
18. Weber A, Weber M, Milligan P (2001) Modeling epidemics caused by respiratory syncytial virus (RSV). *Math Biosci* 172: 95–113. doi: 10.1016/s0025-5564(01)00066-9
19. Respiratory Syncytial Virus (RSV) Infection-Cause. (n.d.). Available: <http://www.webmd.com/lung/tc/respiratory-syncytial-virus-rsv-infection>. Accessed 24 April 2015

Appendix

| States | Total Number of Weeks | Avg Number of Positive Tests |
|----------------------|-----------------------|------------------------------|
| Alabama | 939 | 7.40 |
| Arizona | 977 | 14.90 |
| Arkansas | 967 | 7.01 |
| California | 1047 | 37.67 |
| Colorado | 1049 | 11.68 |
| Connecticut | 951 | 6.67 |
| Delaware | 1008 | 4.24 |
| District of Columbia | 581 | 1.01 |
| Florida | 991 | 25.91 |
| Georgia | 988 | 25.40 |
| Idaho | 475 | 1.39 |
| Illinois | 1030 | 18.43 |
| Indiana | 1048 | 16.05 |
| Iowa | 748 | 3.03 |
| Kansas | 471 | 9.93 |
| Kentucky | 998 | 8.23 |
| Louisiana | 1084 | 20.53 |
| Maine | 432 | 2.37 |
| Maryland | 657 | 10.32 |
| Massachusetts | 879 | 10.35 |
| Michigan | 940 | 7.08 |
| Minnesota | 586 | 21.21 |
| Mississippi | 791 | 2.64 |
| Missouri | 1035 | 37.34 |
| Montana | 995 | 3.34 |
| Nebraska | 1025 | 7.93 |
| Nevada | 904 | 9.54 |
| New Hampshire | 790 | 2.55 |
| New Jersey | 1002 | 10.22 |
| New Mexico | 745 | 4.78 |
| New York | 1049 | 33.26 |
| North Carolina | 904 | 6.27 |
| North Dakota | 895 | 3.29 |
| Ohio | 1016 | 20.81 |
| Oklahoma | 1035 | 8.10 |
| Oregon | 641 | 5.26 |
| Pennsylvania | 494 | 26.89 |
| Rhode Island | 810 | 8.29 |
| South Carolina | 993 | 6.24 |
| South Dakota | 1026 | 11.65 |
| Tennessee | 1034 | 16.79 |
| Texas | 1021 | 63.89 |
| Utah | 746 | 16.81 |
| Vermont | 187 | 2.02 |
| Virginia | 994 | 10.21 |
| Washington | 1057 | 18.16 |
| West Virginia | 1013 | 13.66 |
| Wisconsin | 1035 | 10.88 |
| Wyoming | 771 | 2.71 |

Table S1 Laboratory Data Summary The total number of weekly RSV data reported for each state and the average number of positive RSV tests.

| States | R_0 | b | φ | h |
|----------------------|------|------|-----------|------|
| Alabama | 9.04 | 0.20 | -0.16 | 0.12 |
| Arizona | 8.98 | 0.33 | -0.07 | 0.16 |
| Arkansas | 8.98 | 0.19 | -0.13 | 0.19 |
| California | 8.89 | 0.26 | -0.08 | 0.07 |
| Colorado | 9.17 | 0.24 | -0.04 | 0.18 |
| Connecticut | 9.09 | 0.27 | -0.15 | 0.17 |
| Delaware | 9.20 | 0.26 | -0.14 | 0.38 |
| District of Columbia | 9.13 | 0.17 | -0.12 | 0.07 |
| Florida | 8.92 | 0.12 | -0.29 | 0.14 |
| Georgia | 9.16 | 0.21 | -0.18 | 0.19 |
| Idaho | 8.66 | 0.16 | 0.00 | 0.04 |
| Illinois | 9.01 | 0.22 | -0.11 | 0.10 |
| Indiana | 9.08 | 0.24 | -0.08 | 0.20 |
| Iowa | 9.10 | 0.30 | -0.07 | 0.07 |
| Kansas | 8.91 | 0.23 | -0.09 | 0.12 |
| Kentucky | 9.03 | 0.17 | -0.14 | 0.16 |
| Louisiana | 9.15 | 0.21 | -0.17 | 0.31 |
| Maine | 9.14 | 0.28 | -0.04 | 0.08 |
| Maryland | 9.20 | 0.20 | -0.14 | 0.09 |
| Massachusetts | 9.05 | 0.22 | -0.13 | 0.13 |
| Michigan | 9.06 | 0.27 | -0.07 | 0.05 |
| Minnesota | 9.17 | 0.25 | -0.11 | 0.18 |
| Mississippi | 8.95 | 0.18 | -0.18 | 0.05 |
| Missouri | 9.02 | 0.25 | -0.09 | 0.53 |
| Montana | 9.38 | 0.27 | -0.01 | 0.29 |
| Nebraska | 9.58 | 0.23 | -0.01 | 0.30 |
| Nevada | 9.03 | 0.15 | -0.07 | 0.28 |
| New Hampshire | 9.05 | 0.26 | -0.08 | 0.16 |
| New Jersey | 9.39 | 0.22 | -0.16 | 0.09 |
| New Mexico | 9.19 | 0.27 | -0.04 | 0.11 |
| New York | 9.05 | 0.20 | -0.15 | 0.14 |
| North Carolina | 9.27 | 0.25 | -0.14 | 0.05 |
| North Dakota | 9.40 | 0.19 | -0.01 | 0.34 |
| Ohio | 9.11 | 0.26 | -0.10 | 0.14 |
| Oklahoma | 9.12 | 0.27 | -0.09 | 0.17 |
| Oregon | 9.47 | 0.22 | 0.00 | 0.07 |
| Pennsylvania | 8.91 | 0.20 | -0.15 | 0.10 |
| Rhode Island | 9.15 | 0.26 | -0.13 | 0.61 |
| South Carolina | 9.51 | 0.18 | -0.11 | 0.10 |
| South Dakota | 9.33 | 0.24 | -0.02 | 1.02 |
| Tennessee | 9.07 | 0.20 | -0.14 | 0.23 |
| Texas | 9.00 | 0.24 | -0.15 | 0.16 |
| Utah | 8.52 | 0.27 | -0.02 | 0.22 |
| Vermont | 9.07 | 0.35 | -0.09 | 0.06 |
| Virginia | 9.26 | 0.19 | -0.14 | 0.10 |
| Washington | 9.14 | 0.21 | -0.05 | 0.23 |
| West Virginia | 8.90 | 0.10 | 0.00 | 0.05 |
| Wisconsin | 9.12 | 0.26 | -0.08 | 0.17 |
| Wyoming | 9.02 | 0.16 | -0.06 | 0.31 |

Table S2 Dynamic Model Parameter Estimates Best-fit parameter estimates obtained by minimizing the negative log-likelihood for all 49 states